Hydrostatic pressure dependence of Brillouin frequency shift in polymer optical fibers

Yosuke Mizuno[1*], Heeyoung Lee[1], Neisei Hayashi[2], and Kentaro Nakamura[1]

[1]*Institute of Innovative Research, Tokyo Institute of Technology, Yokohama 226-8503, Japan*
[2]*Research Center for Advanced Science and Technology, The University of Tokyo, Meguro, Tokyo 153-8904, Japan*

*E-mail: ymizuno@sonic.pi.titech.ac.jp

We experimentally investigate the pressure dependence of the Brillouin frequency shift (BFS) in a polymer optical fiber. The BFS dependence on pressure shows a hysteresis, but after several cycles of increasing/decreasing pressure, the hysteresis is mitigated. The pressure dependence coefficient at this state is +4.3 MHz/MPa, the absolute value of which is 5.8 times as large as that of bare silica fibers (the sign is opposite). The reason for this unique behavior is discussed. This result indicates that, by using plastic optical fibers instead of silica fibers, distributed pressure sensing with a higher sensitivity is potentially feasible. © 2018 The Japan Society of Applied Physics

Brillouin scattering in optical fibers has been the subject of extensive research owing to its capability of distributed measurement of strain and temperature.[1–12] To date, glass optical fibers have mainly been used for the sensor heads of Brillouin sensors, but in order to enhance the flexibility (i.e., strain dynamic range), some research groups[13–22] have started to employ polymer optical fibers (POFs) as the sensor heads. One report has proven that sometimes POFs can withstand extremely large strains of more than 100%.[13]

POF-based sensors have another unique feature called strain and thermal "memory" functions,[14,15] with which the information on the applied large strain (or overheat) can be stored owing to their plastic deformation. For instance, if we exploit the strain memory function, we can propose a novel concept: "we need not always place expensive analyzers at the ends of the sensing fibers; after earthquakes, an officer has only to go round with a single interrogator". This concept will extend the application range of fiber-optic sensing technology, which has been limited only to large-scale civil structures owing to its high cost, to small-scale multifamily residences and individual houses. Consequently, for instance, the evacuation period of people after large earthquakes might be shortened, because people can judge rapidly and accurately whether the houses and buildings are severely damaged.

In addition to such memory functions, previous research studies on Brillouin scattering in POFs[16–19] have clarified its potential applicability to large-strain sensing,[17] to high-precision temperature sensing with less sensitivity to strain,[18] and to low-temperature sensing.[19] Distributed strain and temperature sensing has also been demonstrated by three research groups. Minardo et al.[20] and Dong et al.[21] attempted to demonstrate distributed strain and temperature sensing in a POF based on Brillouin optical frequency-domain analysis (BOFDA)[6] and Brillouin optical time-domain analysis (BOTDA),[1] respectively, but the spatial resolution and signal-to-noise ratio (SNR) of their results were not sufficiently high for practical use. In contrast, our group employed Brillouin optical correlation-domain reflectometry (BOCDR)[11] to perform distributed strain and temperature measurement in a POF. A 10-cm-long heated section of a 1.3-m-long POF was detected with a theoretical spatial resolution of 6.0 cm,[22] and further performance improvement of distributed Brillouin sensing using a POF is being conducted from various aspects, one of which is the increase in the number of kinds of measurands. In addition to strain and

temperature, we have experimentally proved that a local loss can also be detected using slope-assisted BOCDR.[23–25]

Here, we focus on pressure sensing based on Brillouin measurement. In bare silica single-mode fibers (SMFs), the Brillouin frequency shift (BFS) is reported to depend linearly on pressure with a coefficient of −0.74 MHz/MPa at 1.55 μm.[26–28] However, the pressure dependence of the BFS in a POF has not been clarified yet. As polymer materials are generally softer than glass materials, the pressure-induced distortion of a POF is anticipated to be larger than that of a silica SMF, which may result in a larger pressure dependence coefficient. Clarifying this point is extremely important as a first step to perform POF-based distributed pressure sensing.

In this work, we experimentally investigated the hydrostatic pressure dependence of the BFS in a POF. As pressure increased, the BFS generally increased; but the case was not so simple. The dependence coefficients were initially different between increasing and decreasing pressures. After three cycles of increasing/decreasing pressure, the BFS dependence on pressure became almost the same, which could be used for practical pressure sensing. The pressure dependence coefficient at this state was +4.3 MHz/MPa, the absolute value of which was 5.8 times as large as that of bare silica SMFs. This result indicates that by using POFs instead of silica SMFs, distributed pressure sensing with a higher sensitivity is potentially feasible in the future.

Light propagating in an optical fiber is partially returned via spontaneous Brillouin scattering. The backscattered Stokes light spectrum is called a Brillouin gain spectrum (BGS),[29] and the central frequency of the BGS is down-shifted from the incident frequency by the amount called a BFS. At 1.55 μm, the BFS of a silica SMF is known to be ~10.8 GHz[29] and that of a perfluorinated graded-index (PFGI-) POF (the only type of POF in which Brillouin scattering has been experimentally observed) is ~2.8 GHz.[16] If temperature change (or strain) is applied to the fiber, the BFS shifts toward a higher or lower frequency according to the fiber core material, in which lies the basic principle of Brillouin temperature (or strain) sensing. The temperature dependence coefficient of the BFS of a PFGI-POF is reported to be −3.2 MHz/K (or −4.1 MHz/K, depending on the fiber structure)[16,19] at 1.55 μm, the absolute value of which is ~3 times that of a silica SMF. Moreover, the strain dependence coefficient of the BFS of a PFGI-POF is −121.8 MHz/%,[16] the absolute value of which is about one-fifth that of a silica SMF. Thus, Brillouin scattering in a PFGI-POF has been
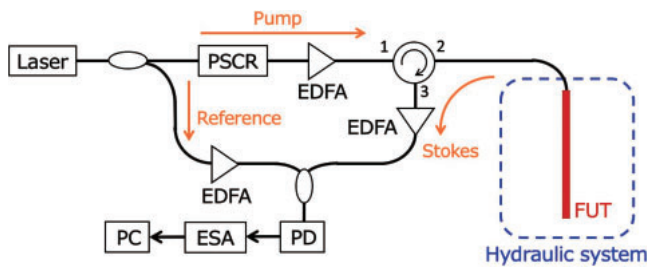
Fig. 1. Experimental setup for investigating the hydrostatic pressure dependence of the BFS in a POF. EDFA, erbium-doped fiber amplifier; ESA, electrical spectrum analyzer; PSCR, polarization scrambler; PD, photodiode.

shown to have a big potential for high-precision temperature sensing with reduced strain sensitivity.

In bare silica SMFs, the BFS is reported to depend on not only strain and temperature but also pressure.[26–28] With increasing pressure, the BFS linearly decreases with a dependence coefficient of −0.74 MHz/MPa at 1.55 μm. This dependence is reported to be similar to that of a bulk silica, and this coefficient is known to originate from the change in longitudinal acoustic velocity rather than from the change in refractive index.[26]

We employed a 3.0-m-long PFGI-POF[30] as a fiber under test (FUT). The POF had a three-layered structure consisting of core, cladding, and overcladding layers (diameters: 50, 70, and 490 μm, respectively). It had a numerical aperture of 0.185, a core refractive index of ~1.35, and a propagation loss of ~0.25 dB/m at 1.55 μm. The core/cladding and over-cladding layers were composed of doped/undoped amorphous perfluorinated polymer and polycarbonate, respectively. The water absorption ratios of these polymers are known to be negligibly low.[31]

Figure 1 schematically shows the experimental setup for investigating the hydrostatic pressure dependence of the BFS in the POF. This setup operates on the basis of self-heterodyne in the same manner as that used for the first observation of Brillouin scattering in a POF.[16] All the optical paths except the FUT are composed of silica SMFs. A laser diode at 1.55 μm with a linewidth of ~1 MHz was used as a light source. Its output was divided into two light beams: pump and reference. The pump light was amplified to ~22 dBm using an erbium-doped fiber amplifier (EDFA) and injected into the FUT. The backscattered Stokes light was amplified to ~1 dBm using another EDFA. The reference light was also amplified to ~1 dBm and coupled with the Stokes light for heterodyne detection. Using a polarization scrambler (PSCR), the polarization state was averaged to increase the measurement stability. The optical beat signals were converted into electrical signals using a photodiode (PD) and observed using an electrical spectrum analyzer (ESA). When the BGS was acquired from the ESA to a personal computer, averaging was performed 1000 times for precise measurement. The raw data around the BGS peak was fitted by a Gaussian curve to deduce the BFS.

A hydraulic system was used to apply pressure on the POF from 0.1 MPa (atmospheric) to 0.6 MPa. With a pump, water was pushed through a one-way valve to a sealed hydraulic tank (diameter: 250 mm; height: 450 mm), in which the FUT was placed. The pressure was measured using a commercial pressure gauge, and a hand valve was used to release the
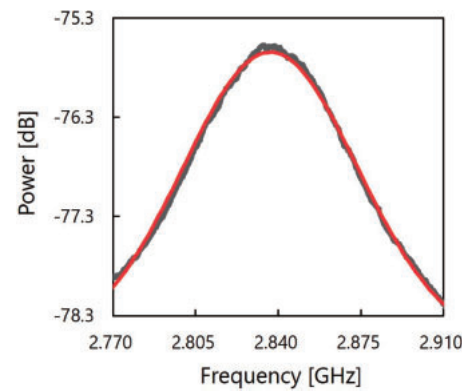

Fig. 2. Example of raw and fitted BGS. Data of the 4th cycle (0.3 MPa; increasing). The solid curve is a Gaussian fit.
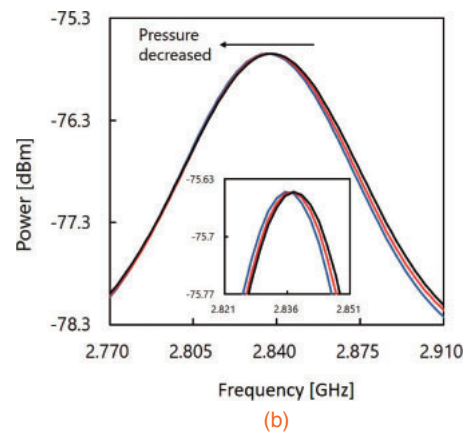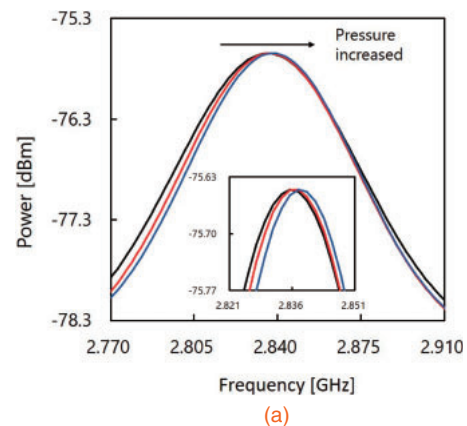

Fig. 3. Examples of fitted BGS dependence on (a) increasing pressure (0.1, 0.3, and 0.5 MPa) and (b) decreasing pressure (0.6, 0.4, and 0.2 MPa). Data of the 4th cycle. The insets show the magnified views around the peaks.

pressure if necessary. The silica SMF connected to the POF (via butt-coupling)[16] was passed through a hole on the tank cover. The water temperature was ~10 °C.

First, the validity of the Gaussian fitting of the measured BGS was verified. An example is shown in Fig. 2, where the raw BGS was obtained when the pressure was 0.3 MPa (4th cycle; refer to the following paragraphs for the meaning of "cycle"). The raw data around the BGS peak was well fitted with the Gaussian curve, leading to the objective acquisition of the BFS. In the same way, examples of the pressure dependence of the BGS (4th cycle) are shown in Figs. 3(a) and 3(b). As the pressure increased (or decreased), the BGS also increased (or decreased).
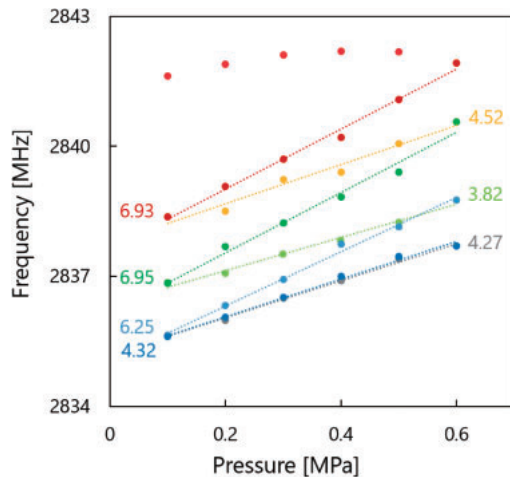
Fig. 4. Pressure dependence of the BFS in the POF. The pressure was increased and then decreased 4 times. The dotted lines are linear fits of each process. The numbers indicated next to each trend are the pressure dependence coefficients (unit: MHz/MPa).

Subsequently, the BFS dependence on pressure was measured, as shown in Fig. 4. Interestingly, the dependence coefficient was initially different between increasing and decreasing pressures; therefore, we performed the same measurement while repeating the increasing/decreasing processes of the pressure 4 times. At each data plot, we waited ~5 min for the BGS to become stable.

When the pressure was first applied to the POF, the BFS was not stable and its pressure dependence was not linear. This instability might be caused by the unideal interface between the core/cladding and overcladding layers (the fabrication technique for PFGI-POFs has not matured yet), whereas the pressure dependence is relatively small probably because the overcladding layer absorbs most of the pressure and the pressure applied to the core/cladding layer itself is low.

After the measurement at 0.6 MPa was finished, the applied pressure was reduced to 0.1 MPa (atmospheric); during this process, the BGS was relatively stable and the BFS decreased almost linearly with decreasing pressure with a coefficient of 6.93 MHz/MPa. The stability was improved probably because the interface between the core/cladding and overcladding layers became relatively uniform with pressing. The larger dependence coefficient might originate from the plastic deformation of the POF. In this case, plastic deformation has two types, one is radial (i.e., diameter change) and the other is longitudinal (i.e., length change). If the diameter of the core is reduced by pressing, the density of the core increases, leading to the increases in acoustic velocity and in BFS (because the material becomes less soft).[32] In contrast, if the POF length increases (or the POF is strained), the BFS decreases (through the reduction in Young's modulus).[18] Considering that the BFS is lowered compared with its initial value, plastic deformation in the longitudinal direction (elongation of the POF) appears to be the reason for this difference between the increasing and decreasing processes.

In the 2nd cycle of measurement, the BGS was relatively stable even when pressure increased. This may verify our speculation regarding the instability in the first cycle. The coefficients were 4.52 and 6.95 MHz/MPa for the increasing

and decreasing processes, respectively. In the 3rd cycle, the coefficients were 3.82 and 6.25 MHz/MPa for the increasing and decreasing processes, respectively. As a cycle is added, the coefficients tended to decrease regardless of the process. This behavior is somewhat in analogy with that for the thermal treatment of intensity-based sensors using polymethyl methacrylate POFs,[33] in which five cycles of heating/cooling processes led to constant sensing performance.

In the 4th cycle, the BFS dependence on pressure showed almost no difference between the increasing and decreasing processes. This state with almost no hysteresis could be exploited for practical pressure sensing. The pressure dependence coefficient at this state was ~4.3 MHz/MPa. The sign was opposite to that of bare silica SMFs, the reason for which is that the increased density of the pressed polymer material leads to the increased acoustic velocity and that this effect is more dominant than that in the case of silica SMFs. What is important for sensing application is the absolute value of the dependence coefficient, which was 5.8 times as large as that of silica SMFs,[26] indicating that Brillouin sensing with high pressure sensitivity could be achieved by using POFs. The decrease in BFS at zero pressure corresponds to an approximately 0.1% increase in POF length,[18] which was difficult to precisely measure experimentally because of the flexibility of the POF and the thermal expansion caused by temperature change. Note that the trend in the 5th cycle was comparable to that in the 4th cycle.

Finally, we discuss the methods for further enhancing the pressure sensitivity of the BFS in a POF. One easy method is to use POFs with a thinner overcladding layer or a larger core. Then, the external pressure will be more directly applied to the core. Another method is to remove the overcladding layer of the POF. Such POFs without overcladding layers are not commercially available, and some research groups tried to etch the overcladding layer selectively using chloroform,[34,35] but it generally induces considerable loss; further study on this point is needed. Yet another method is to employ POFs after the so-called "BFS hopping" effect caused by a large strain,[32] with which the outer diameter is reduced by 0.8 times (with a jump of the BFS to ~3.2 GHz). This means that the overcladding layer is thinned, and a higher pressure sensitivity is anticipated. Note that such a high pressure sensitivity has been achieved using Brillouin dynamic gratings (BDGs);[36,37] but compared with the relatively simple BFS measurement, the BDG measurement requires a far more complicated setup, and the FUT generally needs to be a polarization-maintaining fiber.

In conclusion, the hydrostatic pressure dependence of the BFS in a POF was experimentally investigated. The BFS dependence on pressure showed a hysteresis, the reason for which appears to be the unideal interface between the core/cladding and overcladding layers, and the plastic deformation in both radial and longitudinal directions. After three cycles of increasing/decreasing pressure, the hysteresis was mitigated. The pressure dependence coefficient at this state was +4.3 MHz/MPa. Compared with the case of silica SMFs, the sign was opposite and the absolute value was 5.8 times as large. In addition, we discussed some methods for further enhancing the pressure sensitivity. Further increase in maximal applied pressure may cause a new phenomenon,[32] which should be studied in the future. Thus, we believe that

this work will open up a new way to fiber-optic distributed pressure sensing with higher sensitivity.

1) T. Horiguchi and M. Tateda, J. Lightwave Technol. **7**, 1170 (1989).
2) T. Kurashima, T. Horiguchi, H. Izumita, S. Furukawa, and Y. Koyamada, IEICE Trans. Commun. **E76-B**, 382 (1993).
3) A. Motil, A. Bergman, and M. Tur, Opt. Laser Technol. **78**, 81 (2016).
4) A. Denisov, M. A. Soto, and L. Thévenaz, Light: Sci. Appl. **5**, e16074 (2016).
5) A. Lopez-Gil, M. A. Soto, X. Angulo-Vinuesa, A. Dominguez-Lopez, S. Martin-Lopez, L. Thévenaz, and M. Gonzalez-Herraez, Opt. Express **24**, 17200 (2016).
6) D. Garus, K. Krebber, F. Schliep, and T. Gogolla, Opt. Lett. **21**, 1402 (1996).
7) A. Minardo, R. Bernini, R. Ruiz-Lombera, J. Mirapeix, J. M. Lopez-Higuera, and L. Zeni, Opt. Express **24**, 29994 (2016).
8) K. Hotate and T. Hasegawa, IEICE Trans. Electron. **E83-C**, 405 (2000).
9) Y. H. Kim, K. Lee, and K. Y. Song, Opt. Express **23**, 33241 (2015).
10) E. Preter, D. Ba, Y. London, O. Shlomi, Y. Antman, and A. Zadok, Opt. Express **24**, 27253 (2016).
11) Y. Mizuno, W. Zou, Z. He, and K. Hotate, Opt. Express **16**, 12148 (2008).
12) Y. Mizuno, N. Hayashi, H. Fukuda, K. Y. Song, and K. Nakamura, Light: Sci. Appl. **5**, e16184 (2016).
13) H. Ujihara, N. Hayashi, M. Tabaru, Y. Mizuno, and K. Nakamura, IEICE Electron. Express **11**, 20140707 (2014).
14) K. Nakamura, I. R. Husdi, and S. Ueha, Proc. SPIE **5855**, 807 (2005).
15) K. Minakawa, N. Hayashi, Y. Mizuno, and K. Nakamura, IEEE Photonics
Technol. Lett. **27**, 1394 (2015).
16) Y. Mizuno and K. Nakamura, Appl. Phys. Lett. **97**, 021103 (2010).
17) N. Hayashi, Y. Mizuno, and K. Nakamura, Opt. Express **20**, 21101 (2012).
18) Y. Mizuno and K. Nakamura, Opt. Lett. **35**, 3985 (2010).
19) K. Minakawa, N. Hayashi, Y. Shinohara, M. Tahara, H. Hosoda, Y. Mizuno, and K. Nakamura, Jpn. J. Appl. Phys. **53**, 042502 (2014).
20) A. Minardo, R. Bernini, and L. Zeni, IEEE Photonics Technol. Lett. **26**, 387 (2014).
21) Y. Dong, P. Xu, H. Zhang, Z. Lu, L. Chen, and X. Bao, Opt. Express **22**, 26510 (2014).
22) N. Hayashi, Y. Mizuno, and K. Nakamura, J. Lightwave Technol. **32**, 3999 (2014).
23) H. Lee, N. Hayashi, Y. Mizuno, and K. Nakamura, IEEE Photonics J. **8**, 6802807 (2016).
24) H. Lee, N. Hayashi, Y. Mizuno, and K. Nakamura, Opt. Express **24**, 29190 (2016).
25) H. Lee, N. Hayashi, Y. Mizuno, and K. Nakamura, J. Lightwave Technol. **35**, 2306 (2017).
26) H. Gu, H. Dong, G. Zhang, J. He, N. Xu, and D. J. Brown, Chin. Opt. Lett. **10**, 100604 (2012).
27) G. Zhang, H. Gu, H. Dong, L. Li, and J. He, IEEE Sens. J. **13**, 2437 (2013).
28) S. L. Floch and P. Cambon, Opt. Commun. **219**, 395 (2003).
29) G. P. Agrawal, *Nonlinear Fiber Optics* (Academic, New York, 2001).
30) Y. Koike and M. Asai, NPG Asia Mater. **1**, 22 (2009).
31) S. Ando, T. Matsuura, and S. Sasaki, Chemtech **24**, 20 (1994).
32) N. Hayashi, K. Minakawa, Y. Mizuno, and K. Nakamura, Appl. Phys. Lett. **105**, 091113 (2014).
33) N. Zhong, Q. Liao, X. Zhu, M. Zhao, Y. Huang, and R. Chen, Sci. Rep. **5**, 11508 (2015).
34) R. Gravina, G. Testa, and R. Bernini, Sensors **9**, 10423 (2009).
35) N. Hayashi, Y. Mizuno, and K. Nakamura, Electron. Lett. **49**, 1630 (2013).
36) Y. H. Kim, H. Kwon, J. Kim, and K. Y. Song, Opt. Express **24**, 21399 (2016).
37) L. Teng, H. Zhang, Y. Dong, D. Zhou, T. Jiang, W. Gao, Z. Lu, L. Chen, and X. Bao, Opt. Lett. **41**, 4413 (2016).